



HAL
open science

Cryo-electron microscopy of the chromatin fiber

Ramachandran Boopathi, Stefan Dimitrov, Ali Hamiche, Carlo Petosa, Jan Bednar

► **To cite this version:**

Ramachandran Boopathi, Stefan Dimitrov, Ali Hamiche, Carlo Petosa, Jan Bednar. Cryo-electron microscopy of the chromatin fiber. *Current Opinion in Structural Biology*, 2020, 64, pp.97-103. 10.1016/j.sbi.2020.06.016 . hal-02947617

HAL Id: hal-02947617

<https://hal.univ-grenoble-alpes.fr/hal-02947617>

Submitted on 29 Aug 2022

HAL is a multi-disciplinary open access archive for the deposit and dissemination of scientific research documents, whether they are published or not. The documents may come from teaching and research institutions in France or abroad, or from public or private research centers.

L'archive ouverte pluridisciplinaire **HAL**, est destinée au dépôt et à la diffusion de documents scientifiques de niveau recherche, publiés ou non, émanant des établissements d'enseignement et de recherche français ou étrangers, des laboratoires publics ou privés.

Cryo-electron microscopy of the chromatin fiber

Ramachandran Boopathi^{1,3}, Stefan Dimitrov^{1,5}, Ali Hamiche², Carlo Petosa³ and Jan Bednar^{1,4*}

¹Université Grenoble Alpes, CNRS UMR 5309, INSERM U1209, Institute for Advanced Biosciences (IAB), Site Santé – Allée des Alpes, 38700 La Tronche, France

²Département de Génomique Fonctionnelle et Cancer, Institut de Génétique et Biologie Moléculaire et Cellulaire (IGBMC)/Université de Strasbourg/CNRS/INSERM, 67404 Illkirch Cedex, France.

³Université Grenoble Alpes, CNRS, CEA, Institut de Biologie Structurale (IBS), 38000 Grenoble, France

⁴Laboratory of the Biology and Pathology of the Eye, Institute of Biology and Medical Genetics, First Faculty of Medicine, Charles University and General University Hospital in Prague, Albertov 4, 128 00 Prague 2, Czech Republic

⁵Izmir Biomedicine and Genome Center, Dokuz Eylul University Health Campus, Balçova, Izmir 35330, Turkey

*Corresponding author : jan.bednar@univ-grenoble-alpes.fr

Abstract

The three-dimensional (3D) organization of chromatin plays a crucial role in the regulation of gene expression. Chromatin conformation is strongly affected by the composition, structural features and dynamic properties of the nucleosome, which in turn determine the nature and geometry of interactions that can occur between neighboring nucleosomes. Understanding how chromatin is spatially organized above the nucleosome level is thus essential for understanding how gene regulation is achieved. Towards this end, great effort has been made to understand how an array of nucleosomes folds into a regular chromatin fiber. This review summarizes new insights into the 3D structure of the chromatin fiber that were made possible by recent advances in cryo-electron microscopy.

Introduction

The standard textbook view of eukaryotic chromatin depicts a hierarchical organization in which nucleosomes arranged along the DNA as 11-nm "beads on a string" fold into more

compact 30-nm fibers, which in turn fold into higher-order structures of increasing complexity [1]. However, the pertinence of this textbook view to chromatin organization *in vivo* is a matter of debate. Numerous studies failed to detect 30-nm fibers in many eukaryotic nuclei, where chromatin appears to form irregularly folded chains [2-6] with zigzag features [7, 8]. Nevertheless, in some terminally differentiated cells the presence of well-defined 30-nm fibers is well-established [9-12], suggesting a role for such structures in transcriptionally inactive chromatin. In any event, studies of the organization and compaction/decompaction mechanism of the 30 nm fiber remain a powerful means for discovering structural properties of chromatin that can shed valuable light on the molecular mechanisms regulating gene expression and other DNA-templated processes. This review will focus on cryo-electron microscopy (cryo-EM) studies that relate to regular chromatin fibers with a periodic structure (**Table 1**). For studies of the irregular, more dynamic chromatin structures observed in many cells, readers are referred to a recent review [13].

Early EM studies of chromatin

Since its discovery the chromatin fiber has been the focus of intense study by diverse techniques. Studies were performed either on isolated chromatin or *in situ* using isolated nuclei or whole cells. Pioneering electron microscopy (EM) studies of the chromatin fiber by Klug and colleagues [14, 15] revealed that chromatin fibers isolated from nuclei under physiological ionic conditions (and containing the linker histone, discussed below) had a diameter of about 30 nm and a density of approximately 6-8 nucleosomes per 11 nm along the fiber axis. These and subsequent studies led to the emergence of two distinct structural models: a one-start helix (solenoid) with a consecutive arrangement of nucleosomes [14] and a two-start zigzag helicoidal structure [16-19]. Later, the coexistence of one-and two-start structures within the same fiber [20] and a polymorphic fiber model incorporating nucleosome repeat length (NRL) variability [21] were also proposed.

Higher order chromatin organization was shown to be critically dependent on the presence of the linker histone (named H1 or H5) [1, 22], which associates at the nucleosomal DNA entry/exit site to induce the formation of an apposed linker DNA stem motif [23-25]. However, despite this important early progress, because of the conformational variability of the chromatin fiber and the many environmental factors that affect its degree of compaction, the limitations of standard EM techniques were soon recognized. In particular, adsorption to the flat EM grid surface altered the 3D conformation of the fiber, and the need for dehydration made the control of ionic environment impossible. It therefore became obvious that analysis of the vitrified hydrated state by cryo-EM would be the method of choice for investigating the structure of the fiber.

Cryo-EM of isolated chromatin fibers

Initial attempts to analyse chromatin by cryo-EM date to 1986 when images of vitrified SV40 minichromosomes isolated from infected mammalian cells were first recorded [26]. Detailed cryo-EM studies of the chromatin fiber were later performed by Woodcock's group [24, 27, 28], including the first use of cryo-EM tomography (cryo-ET) [29]. The organization and conformation of the chromatin fiber are determined by various factors. The most important of these are: the isoform and relative amount of the linker histone bound [30], the ionic conditions, the composition of the core histones (presence of specific histone variants), the type and degree of posttranslational modifications [31], and the length of the DNA linker [32] and of core histone tails [33, 34]. Thus, native chromatin fibers isolated from nuclei are poorly suited for high resolution studies by single particle analysis (SPA) but are suitable for analysis by cryo-ET. For SPA, most recent studies use reconstituted chromatin arrays with a rigorously defined composition. It should be noted that the reliable and well controlled reconstitution of chromatin arrays only became possible following the discovery of the strongly positioning 601 DNA sequence [35] and the introduction of improved linker histone association procedures [25, 36].

Role of the linker histone

A major factor affecting the fold of the chromatin fiber is the linker histone: whereas depletion of the linker histone yields fibers with an erratic appearance, fibers associated with this histone appear highly regular in structure [15]. Linker histone isoforms include 11 mammalian H1 subtypes and the avian erythrocyte variant H5. These are characterized by a central globular domain flanked by intrinsically disordered N- and C-terminal domains [1]. The C-terminal domain is highly positively charged and largely responsible for the condensation state of the chromatin fiber [25, 34]. The linker histone content in different cell types ranges between 0.5 and 1 per nucleosome and this number correlates linearly with the nucleosome repeat length (NRL) [37]. Studies of reconstituted nucleosome arrays revealed that the degree of compaction and 3D conformation of the chromatin fiber varies with different linker histone stoichiometries and NRLs [38]. Post-translational modifications of the linker histone have also been shown to alter the degree of chromatin compaction [39, 40].

Efforts to determine the binding configuration of linker histones within the nucleosome have led to divergent conclusions concerning both their location and orientation [41-44]. In 2017, Bednar *et al.* [45] reported the structure of a 197 bp nucleosome associated with full-length H1 (isoforms H1.0 and H1.5) at 6.3 Å resolution determined by cryo-EM and SPA (Figure 1A). The structure revealed the H1 globular domain positioned on the nucleosomal dyad axis and in contact with both DNA arms ("on-dyad" binding mode), in agreement with the crystal structure of a 167 bp nucleosome bound to the H5 globular domain [46]. 3D classification also revealed an alternate, more open conformation in which the globular domain contacted only one DNA arm. This study showed how the binding of H1 drew the two linker DNA arms

together and reduced their dynamic flexibility, thereby limiting the conformational landscape available to the chromatin fiber and its possible modes of compaction. Moreover, cryo-EM was crucial in revealing that the H1.0 C-terminal domain associates with only a single DNA linker arm, imparting a strong degree of asymmetry to the nucleosome that is likely to have implications for higher-order chromatin structure.

The histone H3 variant CENP-A

CENP-A, a variant of histone H3, marks centromeres epigenetically and is essential for mitotic fidelity. CENP-A nucleosomes recruit centromeric proteins during kinetochore assembly, but their influence on the higher-order structure of centromeric chromatin is poorly understood. Cryo-EM analysis of CENP-A nucleosomes revealed that, compared to H3, CENP-A induces more open linker arm conformations and larger DNA end orientation fluctuations [47], consistent with previous reports that the DNA ends of CENP-A nucleosomes have higher dynamic flexibility [48]. This enhanced flexibility was shown to be essential for proper kinetochore formation and a source of local irregularity in chromatin fiber folding [47]. To shed light on the impact of CENP-A on higher-order chromatin structure, Takizawa *et al.* used cryo-EM to study tri-nucleosomes composed of a central CENP-A nucleosome flanked on either side by an H3 nucleosome [49]. These H3-(CENP-A)-H3 tri-nucleosomes adopted a configuration remarkably less twisted than that observed for H3-H3-H3 tri-nucleosomes. Hypothetical chromatin fiber models based on these structures suggested that an untwisted CENP-A conformation embedded in an H3 nucleosomal fiber would yield a highly exposed CENP-A nucleosome [49]. This, in combination with the experimental data showing that histone H1 is not able to bind to the CENP-A nucleosome [47], suggest that CENP-A incorporation may induce the local opening of an otherwise compact folded chromatin fibre, providing insights into how CENP-A enables the recruitment of centromeric proteins during kinetochore assembly. Nucleosomes containing other histone variants with features resembling those of CENP-A might similarly affect chromatin fiber folding [50].

Oligonucleosome arrays

In vitro reconstituted oligonucleosome arrays are useful for investigating the structure of the 30 nm chromatin fiber as they form well-defined molecular objects suitable for single particle analysis (SPA). However, as the size of the array increases so do the complexity of oligonucleosome preparation and the occurrence of irregularities within the fiber. Robinson and colleagues [51] reconstituted long nucleosome arrays (n=22 to 72) with a varying NRL (from 177 to 237 in steps of 10 bp) in the presence of linker histone H5 and analyzed their structures by negative-stain EM and cryo-EM. Two classes of highly compact fiber structure (11 or 15 nucleosomes per 11 nm versus the more usual 6-8) were observed. This had an essentially constant diameter of either ~33 or ~44 nm, depending on whether arrays had NRLs of 177-207 or 217-237 bp, respectively. These observations argued against a two-start helical

fiber structure and led the authors to propose a one-start interdigitated solenoid model (Figure 2A).

By contrast, SPA performed by Song *et al.* on reconstituted nucleosome arrays comprising 12×177, 12×187 or 24×187 bp repeats and bound to a linker histone (human isoform H1.4) revealed a chromatin fiber structure with a two-start twisted helical organization at 11 Å resolution (Figure 2B) [52]. These fibers exhibited a left-handed topology with a canonical packing density (6.1-6.4 nucleosomes/11 nm) and a diameter of approximately 27 or 30 nm for NRLs of 177 and 187 bp, respectively. Strikingly, the basic repeating motif of these fibers is a tetranucleosomal unit that closely resembles the crystal structure of a tetranucleosome reconstituted *in vitro* in the absence of a linker histone [53]. In addition, these fibers exhibited an off-dyad binding mode for the H1.4 linker histone (Figure 1B). The use in this study [52] of a low ionic strength buffer and of chemical (glutaraldehyde) fixation (reported to perturb nucleosome array conformation [54]) raises the possibility that a different fiber conformation may prevail under physiological conditions.

Garcia-Saez *et al.* combined X-ray crystallography and cryo-EM to investigate H1-bound 6- and 12-nucleosome arrays reconstituted in ionic conditions that favor incomplete chromatin condensation [55]. The 9.7 Å resolution crystal structure of a 6×187 bp array bound to *Xenopus laevis* linker histone H1.0b revealed a flat two-start helix with a ladder-like conformation. While the diameter (~32 nm) of this helix was typical, the nucleosome packing density (3.9 nucleosomes/11 nm) was roughly only half that of a canonical 30-nm fibre. DNA footprinting analysis suggested that the H1.0b linker histone adopted an on-dyad binding mode, similar to that observed in the isolated nucleosome [45, 46]. Interestingly, an increase in Mg²⁺ concentration shifted arrays to adopt a twisted conformation resembling that observed by Song *et al.* [52], suggesting that the ladder-like conformation represents an untwisted form of the canonical 30-nm fibre (Figure 3A and B).

Isolated native chromatin fibers

The 3D structure of native chromatin fibers has primarily been addressed by cryo-ET, as the high conformational variability of these fibers is a major obstacle for SPA. Scheffer and colleagues [56] determined the structure of native chromatin fibers isolated from chicken erythrocytes and starfish sperm in different ionic conditions and states of compaction (Figure 3C and D). Despite an important difference in linker DNA length, both types of folded fibers showed regions in which nucleosomes stacked with their dyad axes aligned, forming a “double-track” conformation resembling that reported by Garcia-Saez *et al.* [55]. Cryo-ET has also been used to study local decompaction of the chromatin fibre, an important transition allowing greater accessibility of the DNA. Cryo-ET of chromatin extracted from human MCF7 cells [57] revealed transitions between the 30-nm fiber and lower order bead-on-a-string nucleosomal arrays that involved a hierarchical branching structure. Analysis of these

structures revealed that some of the fibers formed helical ribbons resembling *in vitro* reconstituted chromatin, while others were irregularly twisted together.

Cryo-EM of the chromatin fiber *in situ*

Until recently, cryo-EM studies of chromatin *in situ* were limited to the preparation of frozen hydrated sections followed by single frame imaging or cryo-ET. Single frame imaging revealed the existence of 30-nm chromatin fibers in swollen chicken erythrocyte nuclei [11], whereas imaging of HeLa cells revealed irregularly folded chromatin fibers lacking any obvious 30-nm organization [2]. Cryo-ET confirmed the existence of the 30-nm chromatin fiber in chicken erythrocytes [12], revealing a left-handed two-start helix with approximately 6.5 nucleosomes per 11 nm and no interdigitation. However, an irregular chromatin organization was observed by cryo-ET even at the level of short oligonucleosomes in HeLa cells [58] and *S. pombe* [59], suggesting that the 30-nm fiber is a specific chromatin arrangement restricted to particular cellular contexts.

Conclusions

The intriguing diversity of chromatin fiber structures cited in this review highlights the great structural plasticity of chromatin. Diverse organisms and cell types exhibit great differences in chromatin at all scales of organization, ranging from the volume and localization of heterochromatin and euchromatin fractions to the type, extent and distribution of histone post-translational modifications, histone variants and linker histones incorporated. Thus, in general native chromatin structures originating from different sources are not directly comparable. For this reason, chromatin reconstituted from homogeneous components under well-defined conditions remains an attractive system for studying the conformation and dynamics of chromatin and how these vary in different biochemical environments. While reconstituted nucleosomal arrays may not fully recapitulate the properties of native chromatin fibers, they currently represent the only route to 3D structural information on the fiber at subnanometer resolution. Additional studies of oligonucleosome arrays of varying composition (e.g. histone variants or mutants, linker length etc.) and in different (primarily intermediate) states of compaction are needed to elucidate the detailed folding and unfolding pathways of the chromatin fiber. Nevertheless, great progress can be expected in the near future regarding chromatin fiber structures studied *in situ*. Rapid advances in cryo-ET and sample preparation technology already allow the detection of individual nucleosomes in ultrathin cryo-sections [60], while the use of ultrathin lamellae of frozen hydrated samples prepared by focused ion beam milling combined with scanning EM (FIB-SEM) coupled with cryo-ET [58] brings the technique to a whole new level. In the future this approach should ultimately allow researchers to correlate the *in vivo* and *in vitro* organization of chromatin.

Conflict of interest statement

Nothing declared

Acknowledgment

This work was supported by the Agence Nationale pour la Recherche (ANR-16-CE12-0013, ANR-17-CE11-0019, and ANR-18-CE12-0010), La Ligue Nationale contre le Cancer (Equipe labellisée (to A.H.) USIAS (2015-42), Fondation pour la Recherche Médicale (FRM, “Epigenétique et Stabilité du Genome” Program), Institut National du Cancer, Association pour la Recherche sur le Cancer, Inserm, CNRS, and Université Grenoble Alpes. J.B. acknowledges institutional support (Progres Q25) from Charles University.

References and recommended reading

Papers of particular interest, published within the period of review, have been highlighted as:

- * of special interest
- ** of outstanding interest

1. van Holde, K. (1988). **Chromatin**. Springer-Verlag KG, Berlin, Germany.
2. Eltsov, M., Maclellan, K.M., Maeshima, K., Frangakis, A.S., and Dubochet, J. (2008). **Analysis of cryo-electron microscopy images does not support the existence of 30-nm chromatin fibers in mitotic chromosomes in situ**. *Proc Natl Acad Sci U S A* *105*, 19732-19737.
3. Fussner, E., Strauss, M., Djuric, U., Li, R., Ahmed, K., Hart, M., Ellis, J., and Bazett-Jones, D.P. (2012). **Open and closed domains in the mouse genome are configured as 10-nm chromatin fibres**. *EMBO Rep* *13*, 992-996.
4. Gan, L., Ladinsky, M.S., and Jensen, G.J. (2013). **Chromatin in a marine picoeukaryote is a disordered assemblage of nucleosomes**. *Chromosoma* *122*, 377-386.
5. Nishino, Y., Eltsov, M., Joti, Y., Ito, K., Takata, H., Takahashi, Y., Hihara, S., Frangakis, A.S., Imamoto, N., Ishikawa, T., et al. (2012). **Human mitotic chromosomes consist predominantly of irregularly folded nucleosome fibres without a 30-nm chromatin structure**. *EMBO J* *31*, 1644-1653.
6. Ou, H.D., Phan, S., Deerinck, T.J., Thor, A., Ellisman, M.H., and O'Shea, C.C. (2017). **ChromEMT: Visualizing 3D chromatin structure and compaction in interphase and mitotic cells**. *Science* *357*.
7. Grigoryev, S.A., Bascom, G., Buckwalter, J.M., Schubert, M.B., Woodcock, C.L., and Schlick, T. (2016). **Hierarchical looping of zigzag nucleosome chains in metaphase chromosomes**. *Proc Natl Acad Sci U S A* *113*, 1238-1243.
8. Hsieh, T.H., Weiner, A., Lajoie, B., Dekker, J., Friedman, N., and Rando, O.J. (2015). **Mapping Nucleosome Resolution Chromosome Folding in Yeast by Micro-C**. *Cell* *162*, 108-119.
9. Kizilyaprak, C., Spehner, D., Devys, D., and Schultz, P. (2010). **In vivo chromatin organization of mouse rod photoreceptors correlates with histone modifications**. *PLoS one* *5*, e11039.

10. Langmore, J.P., and Schutt, C. (1980). **The higher order structure of chicken erythrocyte chromosomes in vivo.** *Nature* 288, 620-622.
11. Woodcock, C.L. (1994). **Chromatin fibers observed in situ in frozen hydrated sections. Native fiber diameter is not correlated with nucleosome repeat length.** *J Cell Biol* 125, 11-19.
12. Scheffer, M.P., Eltsov, M., and Frangakis, A.S. (2011). **Evidence for short-range helical order in the 30-nm chromatin fibers of erythrocyte nuclei.** *Proc Natl Acad Sci U S A* 108, 16992-16997.
13. Maeshima, K., Ide, S., and Babokhov, M. (2019). **Dynamic chromatin organization without the 30-nm fiber.** *Curr Opin Cell Biol* 58, 95-104.
14. Finch, J.T., and Klug, A. (1976). **Solenoidal model for superstructure in chromatin.** *Proc Natl Acad Sci U S A* 73, 1897-1901.
15. Thoma, F., Koller, T., and Klug, A. (1979). **Involvement of histone H1 in the organization of the nucleosome and of the salt-dependent superstructures of chromatin.** *J Cell Biol* 83, 403-427.
16. Makarov, V., Dimitrov, S., Smirnov, V., and Pashev, I. (1985). **A triple helix model for the structure of chromatin fiber.** *FEBS Lett* 181, 357-361.
17. Makarov, V.L., Dimitrov, S.I., and Petrov, P.T. (1983). **Salt-induced conformational transitions in chromatin. A flow linear dichroism study.** *Eur J Biochem* 133, 491-497.
18. Williams, S.P., Athey, B.D., Muglia, L.J., Schappe, R.S., Gough, A.H., and Langmore, J.P. (1986). **Chromatin fibers are left-handed double helices with diameter and mass per unit length that depend on linker length.** *Biophys J* 49, 233-248.
19. Worcel, A., Strogatz, S., and Riley, D. (1981). **Structure of chromatin and the linking number of DNA.** *Proc Natl Acad Sci U S A* 78, 1461-1465.
20. Grigoryev, S.A., Arya, G., Correll, S., Woodcock, C.L., and Schlick, T. (2009). **Evidence for heteromorphic chromatin fibers from analysis of nucleosome interactions.** *Proc Natl Acad Sci U S A* 106, 13317-13322.
21. Collepardo-Guevara, R., and Schlick, T. (2014). **Chromatin fiber polymorphism triggered by variations of DNA linker lengths.** *Proc Natl Acad Sci U S A* 111, 8061-8066.
22. Dimitrov, S.I., Russanova, V.R., and Pashev, I.G. (1987). **The globular domain of histone H5 is internally located in the 30 nm chromatin fiber: an immunochemical study.** *EMBO J* 6, 2387-2392.
23. Hamiche, A., Schultz, P., Ramakrishnan, V., Oudet, P., and Prunell, A. (1996). **Linker histone-dependent DNA structure in linear mononucleosomes.** *J Mol Biol* 257, 30-42.
24. Bednar, J., Horowitz, R.A., Grigoryev, S.A., Carruthers, L.M., Hansen, J.C., Koster, A.J., and Woodcock, C.L. (1998). **Nucleosomes, linker DNA, and linker histone form a unique structural motif that directs the higher-order folding and compaction of chromatin.** *Proc Natl Acad Sci U S A* 95, 14173-14178.

25. Syed, S.H., Goutte-Gattat, D., Becker, N., Meyer, S., Shukla, M.S., Hayes, J.J., Everaers, R., Angelov, D., Bednar, J., and Dimitrov, S. (2010). **Single-base resolution mapping of H1-nucleosome interactions and 3D organization of the nucleosome.** *Proc Natl Acad Sci U S A* *107*, 9620-9625.
26. Dubochet, J., Adrian, M., Schultz, P., and Oudet, P. (1986). **Cryo-electron microscopy of vitrified SV40 minichromosomes: the liquid drop model.** *EMBO J* *5*, 519-528.
27. Carruthers, L.M., Bednar, J., Woodcock, C.L., and Hansen, J.C. (1998). **Linker histones stabilize the intrinsic salt-dependent folding of nucleosomal arrays: mechanistic ramifications for higher-order chromatin folding.** *Biochemistry* *37*, 14776-14787.
28. Bednar, J., Horowitz, R.A., Dubochet, J., and Woodcock, C.L. (1995). **Chromatin conformation and salt-induced compaction: three-dimensional structural information from cryoelectron microscopy.** *J Cell Biol* *131*, 1365-1376.
29. Horowitz, R.A., Koster, A.J., Walz, J., and Woodcock, C.L. (1997). **Automated electron microscope tomography of frozen-hydrated chromatin: the irregular three-dimensional zigzag architecture persists in compact, isolated fibers.** *J Struct Biol* *120*, 353-362.
30. Robinson, P.J., and Rhodes, D. (2006). **Structure of the '30 nm' chromatin fibre: a key role for the linker histone.** *Curr Opin Struct Biol* *16*, 336-343.
31. Robinson, P.J., An, W., Routh, A., Martino, F., Chapman, L., Roeder, R.G., and Rhodes, D. (2008). **30 nm chromatin fibre decompaction requires both H4-K16 acetylation and linker histone eviction.** *J Mol Biol* *381*, 816-825.
32. Grigoryev, S.A., and Woodcock, C.L. (2012). **Chromatin organization - the 30 nm fiber.** *Exp Cell Res* *318*, 1448-1455.
33. Dorigo, B., Schalch, T., Bystricky, K., and Richmond, T.J. (2003). **Chromatin fiber folding: requirement for the histone H4 N-terminal tail.** *J Mol Biol* *327*, 85-96.
34. Makarov, V.L., Dimitrov, S.I., Tsaneva, I.R., and Pashev, I.G. (1984). **The role of histone H1 and non-structured domains of core histones in maintaining the orientation of nucleosomes within the chromatin fiber.** *Biochem Biophys Res Commun* *122*, 1021-1027.
35. Lowary, P.T., and Widom, J. (1998). **New DNA sequence rules for high affinity binding to histone octamer and sequence-directed nucleosome positioning.** *J Mol Biol* *276*, 19-42.
36. Huynh, V.A., Robinson, P.J., and Rhodes, D. (2005). **A method for the in vitro reconstitution of a defined "30 nm" chromatin fibre containing stoichiometric amounts of the linker histone.** *J Mol Biol* *345*, 957-968.
37. Woodcock, C.L., Skoultchi, A.I., and Fan, Y. (2006). **Role of linker histone in chromatin structure and function: H1 stoichiometry and nucleosome repeat length.** *Chromosome Res* *14*, 17-25.
38. Routh, A., Sandin, S., and Rhodes, D. (2008). **Nucleosome repeat length and linker histone stoichiometry determine chromatin fiber structure.** *Proc Natl Acad Sci U S A* *105*, 8872-8877.

39. Christophorou, M.A., Castelo-Branco, G., Halley-Stott, R.P., Oliveira, C.S., Loos, R., Radzsheuskaya, A., Mowen, K.A., Bertone, P., Silva, J.C., Zernicka-Goetz, M., et al. (2014). **Citrullination regulates pluripotency and histone H1 binding to chromatin.** *Nature* 507, 104-108.

40. Li, Y., Li, Z., Dong, L., Tang, M., Zhang, P., Zhang, C., Cao, Z., Zhu, Q., Chen, Y., Wang, H., et al. (2018). **Histone H1 acetylation at lysine 85 regulates chromatin condensation and genome stability upon DNA damage.** *Nucleic Acids Res* 46, 7716-7730.

41. Brown, D.T., Izard, T., and Misteli, T. (2006). **Mapping the interaction surface of linker histone H1(0) with the nucleosome of native chromatin in vivo.** *Nat Struct Mol Biol* 13, 250-255.

42. Fan, L., and Roberts, V.A. (2006). **Complex of linker histone H5 with the nucleosome and its implications for chromatin packing.** *Proc Natl Acad Sci U S A* 103, 8384-8389.

43. Zhou, B.R., Feng, H., Kato, H., Dai, L., Yang, Y., Zhou, Y., and Bai, Y. (2013). **Structural insights into the histone H1-nucleosome complex.** *Proc Natl Acad Sci U S A* 110, 19390-19395.

44. Zhou, Y.B., Gerchman, S.E., Ramakrishnan, V., Travers, A., and Muyldermans, S. (1998). **Position and orientation of the globular domain of linker histone H5 on the nucleosome.** *Nature* 395, 402-405.

45*. Bednar, J., Garcia-Saez, I., Boopathi, R., Cutter, A.R., Papai, G., Reymer, A., Syed, S.H., Lone, I.N., Tonchev, O., Crucifix, C., et al. (2017). **Structure and Dynamics of a 197 bp Nucleosome in Complex with Linker Histone H1.** *Mol Cell* 66, 384-397 e388.

Cryo-microscopy and crystal structures of the H1-bound nucleosome were solved and validated by hydroxyl-radical footprinting and site-directed protein-DNA crosslinking. The globular H1 domain binds the nucleosome dyad and contacts both DNA linkers. The H1 C-terminal domain interacts mainly with a single DNA linker.

46. Zhou, B.R., Jiang, J., Feng, H., Ghirlando, R., Xiao, T.S., and Bai, Y. (2015). **Structural Mechanisms of Nucleosome Recognition by Linker Histones.** *Mol Cell* 59, 628-638.

47. Roulland, Y., Ouararhni, K., Naidenov, M., Ramos, L., Shuaib, M., Syed, S.H., Lone, I.N., Boopathi, R., Fontaine, E., Papai, G., et al. (2016). **The Flexible Ends of CENP-A Nucleosome Are Required for Mitotic Fidelity.** *Mol Cell*.

48. Tachiwana, H., Kagawa, W., Shiga, T., Osakabe, A., Miya, Y., Saito, K., Hayashi-Takanaka, Y., Oda, T., Sato, M., Park, S.Y., et al. (2011). **Crystal structure of the human centromeric nucleosome containing CENP-A.** *Nature* 476, 232-235.

49*. Takizawa, Y., Ho, C.H., Tachiwana, H., Matsunami, H., Kobayashi, W., Suzuki, M., Arimura, Y., Hori, T., Fukagawa, T., Ohi, M.D., et al. (2020). **Cryo-EM Structures of Centromeric Tri-nucleosomes Containing a Central CENP-A Nucleosome.** *Structure* 28, 44-53 e44.

The studied centromeric trinucleosome (H3-CA-H3) contained a central CENP-A nucleosome flanked by two conventional H3 nucleosomes, mimicking the organization of centromeric chromatin. The cryo-EM structure of the H3-CA-H3 nucleosome shows that the centrally positioned CENP-A nucleosome disrupts the continuous alignment of H3 nucleosomes and is accessible for binding CENP-C, CENP-N and CENP-B.

50. Syed, S.H., Boulard, M., Shukla, M.S., Gautier, T., Travers, A., Bednar, J., Faivre-Moskalenko, C., Dimitrov, S., and Angelov, D. (2009). **The incorporation of the novel histone variant H2AL2 confers unusual structural and functional properties of the nucleosome.** *Nucleic Acids Res* 37, 4684-4695.

51. Robinson, P.J., Fairall, L., Huynh, V.A., and Rhodes, D. (2006). **EM measurements define the dimensions of the "30-nm" chromatin fiber: evidence for a compact, interdigitated structure.** *Proc Natl Acad Sci U S A* 103, 6506-6511.

52**. Song, F., Chen, P., Sun, D., Wang, M., Dong, L., Liang, D., Xu, R.M., Zhu, P., and Li, G. (2014). **Cryo-EM study of the chromatin fiber reveals a double helix twisted by tetranucleosomal units.** *Science* 344, 376-380.

This cryo-EM study yielded the first 3D structure of a nucleosome array at nanometer resolution. The structure reveals a 30-nm chromatin fiber with a twisted helical zigzag conformation organized as repeating tetranucleosomal units. The H1 linker histone adopts an off-dyad binding mode.

53. Schalch, T., Duda, S., Sargent, D.F., and Richmond, T.J. (2005). **X-ray structure of a tetranucleosome and its implications for the chromatin fibre.** *Nature* 436, 138-141.

54. Zhou, B.R., Jiang, J., Ghirlando, R., Norouzi, D., Sathish Yadav, K.N., Feng, H., Wang, R., Zhang, P., Zhurkin, V., and Bai, Y. (2018). **Revisit of Reconstituted 30-nm Nucleosome Arrays Reveals an Ensemble of Dynamic Structures.** *J Mol Biol* 430, 3093-3110.

55**. Garcia-Saez, I., Menoni, H., Boopathi, R., Shukla, M.S., Soueidan, L., Noirclerc-Savoye, M., Le Roy, A., Skoufias, D.A., Bednar, J., Hamiche, A., et al. (2018). **Structure of an H1-Bound 6-Nucleosome Array Reveals an Untwisted Two-Start Chromatin Fiber Conformation.** *Mol Cell* 72, 902-915 e907.

Crystallographic and cryo-EM studies of an H1-bound 6-nucleosome array were combined with biophysical and novel biochemistry approaches. The structure revealed a flat two-start helix with a nucleosome packing density half that of a twisted 30 nm fiber. Histone H1 adopts an on-dyad binding mode. Conversion of the flat helix to a compact twisted conformation induced by changes in the ionic environment implicate the flat structure as an assembly intermediate of the 30 nm fiber.

56. Scheffer, M.P., Eltsov, M., Bednar, J., and Frangakis, A.S. (2012). **Nucleosomes stacked with aligned dyad axes are found in native compact chromatin in vitro.** *J Struct Biol* 178, 207-214.

57. Zhou, Z., Li, K., Yan, R., Yu, G., Gilpin, C.J., Jiang, W., and Irudayaraj, J.M.K. (2019). **The transition structure of chromatin fibers at the nanoscale probed by cryogenic electron tomography.** *Nanoscale* 11, 13783-13789.

58*. Cai, S., Bock, D., Pilhofer, M., and Gan, L. (2018). **The in situ structures of mono-, di-, and trinucleosomes in human heterochromatin.** *Mol Biol Cell* 29, 2450-2457.

The structure, positions and orientation of nucleosomes inside a HeLa cell nucleus were visualized. Sequential nucleosomes are likely to follow irregular paths at the level of oligonucleosomes.

59*. Cai, S., Chen, C., Tan, Z.Y., Huang, Y., Shi, J., and Gan, L. (2018). **Cryo-ET reveals the macromolecular reorganization of *S. pombe* mitotic chromosomes in vivo.** Proc Natl Acad Sci U S A *115*, 10977-10982.

Cryo-electron tomography shows that in *S. pombe* cells chromatin is organized in multimegadalton complexes and pockets free of such complexes.

60*. Eltsov, M., Grewe, D., Lemercier, N., Frangakis, A., Livolant, F., and Leforestier, A. (2018). **Nucleosome conformational variability in solution and in interphase nuclei evidenced by cryo-electron microscopy of vitreous sections.** Nucleic Acids Res *46*, 9189-9200.

Both cryo-EM and tomography of vitreous sections were used to analyze nucleosomes in their native nuclear environment. Multiple conformations of nucleosomes with distinct distances between DNA gyres of the nucleosomes were observed.

Table 1. Oligonucleosomal structures observed using cryo-EM

Reference	Fiber organization observed	Observation	Method used	Chromatin type	Number of nucleosomes x NRL	Histone/ nucleosome source	Ionic conditions
[51]	Compact interdigitated solenoid	<i>In vitro</i>	EM, Cryo-EM	Reconstituted	22 x 177, 47-72 x 177	Native, chicken erythrocytes	1 mM MgCl ₂
[55]	Flat two-start helix	<i>In vitro</i>	Cryo-EM, X-Ray	Reconstituted	6 x 187, 12 x 197	Recombinant, <i>Xenopus laevis</i> core histones, <i>X. laevis</i> H1.0b	0.35-0.6 mM MgCl ₂
[52]	Two start helix (zigzag)	<i>In vitro</i>	Cryo-EM	Reconstituted	12 x 177, 24 x 177 12 x 187	Recombinant, <i>X. laevis</i> core histones, human H1.4	10 mM HEPES, 0.1 mM EDTA in final dialysis buffer
[56]	Irregular fiber, zigzag	<i>In vitro</i>	Cryo-ET	Native Isolated	Arbitrary	Chicken erythrocytes	40 mM NaCl, 1 mM MgCl ₂
	Irregular fiber, zigzag "double track"	<i>In situ, in vitro</i>		Native Isolated	Arbitrary	Starfish sperm	60 mM NaCl, 26 mM KCl
[12]	Short range irregular zigzag	<i>In situ</i>	Cryo-ET	Native	Arbitrary	Chicken erythrocytes	In cell
[59]	No fiber, irregular arrangement	<i>In situ</i>	Cryo-ET	Native	N/A	<i>S. pombe</i>	In cell
[58]	No fiber, irregular arrangement	<i>In situ</i>	Cryo-ET	Native	N/A	HeLa cell	In cell

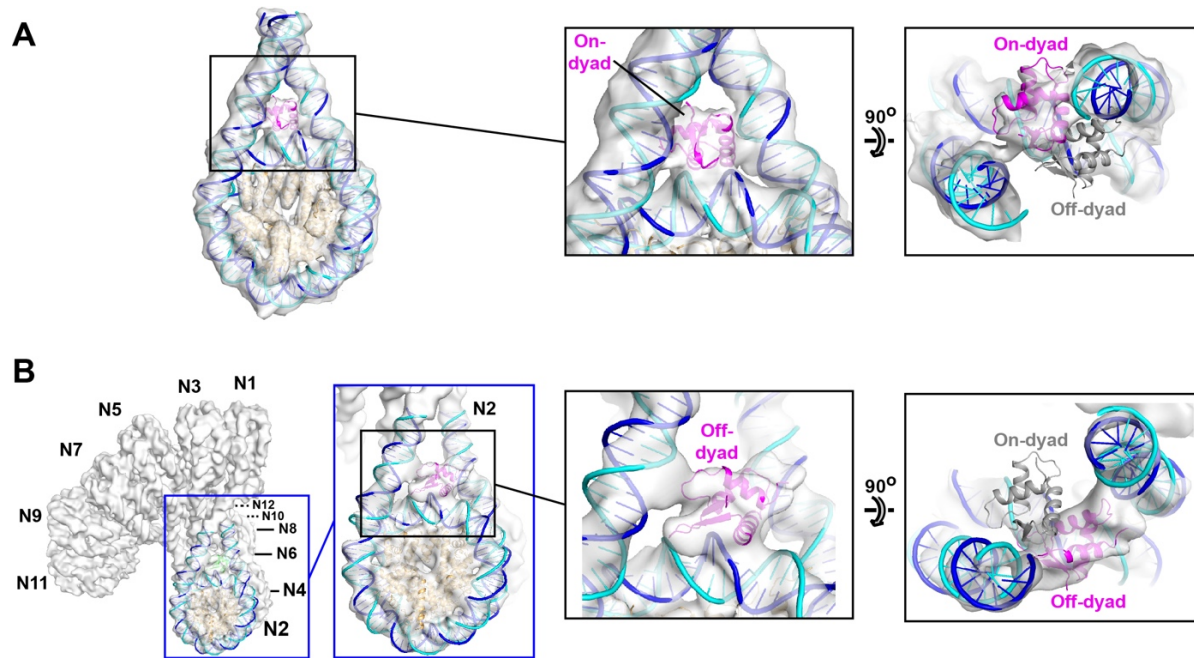


Figure 1. Linker histone binding modes. **A.** Cryo-EM map of a 197-bp nucleosome showing an on-dyad binding mode for the linker histone [41]. **B.** Cryo-EM map of a reconstituted 12-nucleosome array showing an off-dyad binding mode for the linker histone [48].

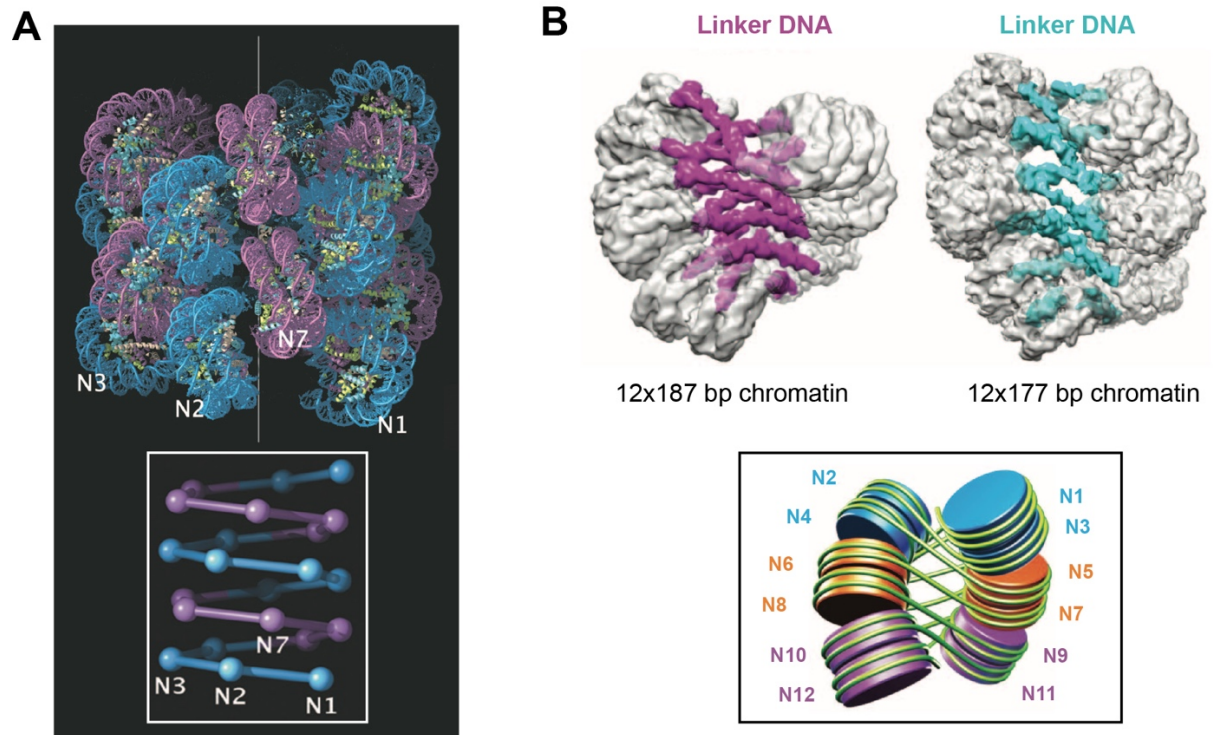


Figure 2. Nucleosome array structures. A. One-start interdigitated solenoid model of chromatin fiber based on EM analysis of long nucleosomal arrays. Figure reproduced from [51]. **B.** Cryo-EM maps of 12-nucleosome arrays showing a two-start helical zigzag organization. Figure reproduced from [52].

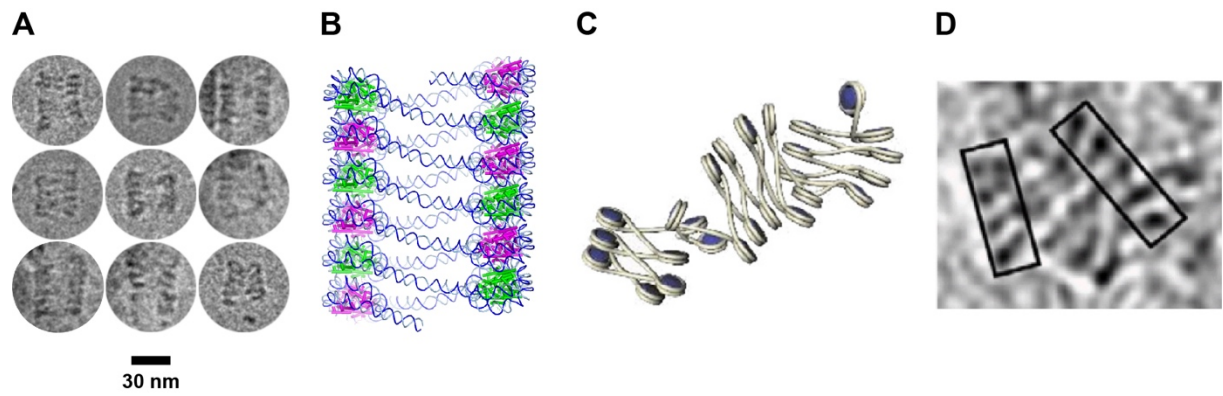


Figure 3. Ladder-like conformation of the chromatin fiber in moderate ionic concentrations.

A. Cryo-EM images of reconstituted 12-nucleosome arrays in 0.35 mM Mg²⁺. **B.** Model of the 12-nucleosome array based on the crystal structure of a hexanucleosome. **C.** Cryo-ET structure of isolated chicken erythrocyte chromatin in 40 mM Na⁺. **D.** Cryo-EM of the same sample in 1 mM Mg²⁺. Note the similarity of the nucleosomal arrangement across the four panels. A,B and C,D reproduced from [50] and [51], respectively.